

Results of VAX/Sigma-9 Compatibility Tests of LWR Camera Images

Myron A. Smith and Kevin M. Hassett

Since the rehosting of IUESIPS to the Goddard VAX 8350 computer on February 16, 1988, the processing of current and archival LWP and SWP images has proceeded routinely. Before the transfer of IUESIPS from the old Xerox Sigma-9 computer could occur, it was necessary to compare the fluxes computed by the two machines for a representative sample of images. A complete description of the tests made on LWP and SWP images is given by J. Nichols-Bohlin (1988). Her results showed that the differences in machine architectures alone, specifically the rounding-off of real numbers by the VAX and the truncation of them by the Sigma, can explain almost all flux differences between the computers. In this article we discuss the results of VAX/Sigma compatibility testing for LWR images. The tests were run on a series of 16 images obtained at both dispersions. One example of every processing scheme was chosen for testing as well as examples of common pathologies that can be introduced by the camera or during the read-out process. Our finding that there are small, predictable flux differences between data processed on the two machines is entirely consistent with Nichols-Bohlin's results from the other two cameras. Consequently, we were able to commence VAX reprocessing of LWR spectra on February 2, 1989.

Three kinds of idiosyncracies were found in the LWR camera that delayed reprocessing of its spectral images: the occurrence of microphonics "pings", a complicated background noise pattern across the camera field, and a peculiar mapping of reseau displacements across the field of this camera. We will give examples below of minor incompatibilities for high and low dispersion images. Before doing so, it may be helpful to classify three types of sources for differences in computed flux by the two machines:

- 1) differences in the computations of fluxes themselves. This comparatively minor discrepancy originates directly from the truncation vs. rounding differences between the Sigma-9 and VAX. The computation of a flux value typically requires about 30 arithmetical operations (Nichols-Bohlin 1987). The error from rounding "random walks" as the square root of the number of operations. In contrast, truncation errors increase linearly with the number of operations and overwhelm round-off errors. For 30 operations truncation errors amount to 1 part in 10^4 , or a maximum of ± 9 FN for MELO and MEHI images. Note that because only a few computations go into constructing the PI file, the maximum discrepancies amount to $\pm 1-2$ FN.

2) differences in the computations of pixel positions. These are typically ± 0.003 pixels between the computers. In the computation of certain spectra the rounding vs. truncation difference causes one or the other of two neighboring pixels to be selected. When this happens, for example, in the MEHI background computations, different fluxes are obviously used. In other kinds of computations (e.g. MELO background) a fractional pixel's flux is computed by a bilinear interpolation of fluxes from the central-most pixel and its three neighbors. The scales of the flux discrepancies in these two cases can be very different, depending upon the flux gradient across the image.

3) the limited size of the Sigma-9's core memory.

HIGH DISPERSION

No unexpected pathologies occurred in the compatibility testing of high dispersion LWR images, and for this reason results are shown only for one representative order of a LWR spectrum. Figures 1-4 show the Sigma-minus-VAX differences in FN for Order 92 of LWR 6257, with the corresponding histogram, for gross, background, net, and ripple-corrected net fluxes. The FN differences for nearly all pixels are less than ± 9 FN. The maximum difference, about 1 part in 10^4 , is remarkably close to predictions (Nichols-Bohlin 1987; Treinish 1980). Please note in Figure 1 the flux difference anomaly at 2507A. This comparatively large difference arises, as explained in #2 above, because the two computers generally compute a slightly different fractional pixel location in the extraction of background flux. For a typical difference of ± 0.003 in real pixel location, the selection of a completely different integral pixel can be expected to happen once or twice per high resolution order. Indeed, the accompanying histogram shows that every other pixel in this order is within the truncation-imposed limit of ± 9 FN. The same explanation holds for the "spike" in the background flux differences in Figure 2. In Figure 3 the background spike is smeared as an artifact of the median/mean filter applied to compute smoothed background fluxes.

Figure 3 also shows a slight tendency of the mean difference to decrease by several FN along the order. This effect is well understood (see Nichols-Bohlin's "high dispersion difference" #2). The slope in the mean arises from an accumulation of truncation errors in the Sigma-9's computation of the smoothed background, specifically from the application of three filters to the raw background fluxes. To understand this, consider that the smoothed flux at each pixel position is computed first by summing the fluxes of 31 adjacent points. When the smoothed flux

for the next pixel position is computed, the first pixel's flux is subtracted from the old sum-bin as a new pixel's flux is added. During each of these add/subtract operations the truncation error is exaggerated by a factor of 31. The error accumulates as more and more pixels are cycled in and out of the bin, resulting in a linear trend in the flux differences. The ripple correction process (division by a sinc-squared function) exaggerates the trend by introducing negative curvature near the edge of the order (Figure 4).

In the course of our testing, we found a wavelength assignment error in the Sigma-9 code which affects the ending-wavelength of high dispersion orders 101-3. The correct (incorrect old) ending-wavelengths are 2313A (2308A), 2290A (2280A), and 2268A (2263A), respectively. Remarkably, because of a coincident sign error in computing the position of the last wavelength, the wavelength assignment error has had no effect on LWR fluxes computed by the Sigma-9 IUESIPS. However, the two errors have been corrected so that the software matched the existing documentation. Neither of these errors occurs in the VAX version of IUESIPS.

LOW DISPERSION

Figure 5-12 shows differences and histograms for the gross, background, net, and absolute net fluxes for a typical low dispersion spectrum, LWR 18150. All the difference plots exhibit a pronounced increase in flux discrepancies toward the middle of the spectral field. For the gross spectrum this pattern is a consequence of the stellar flux exposure and the 10^{-4} truncation error limit. A remarkable feature of this plot is that the pattern persists in the background fluxes (note also Fig. 3 of Nichols-Bohlin 1988). This pattern was present in all the LWR low dispersion spectra tested. The explanation for the background noise pattern is the "bright spot" pathology noted by Nichols-Bohlin, but under a new guise. An exaggerated flux discrepancy occurs whenever a sharp flux gradient exists between adjacent pixels, for example because of a local "bright spot" or cosmic ray hit, or a sharp emission line. In such cases the "flux error" is actually an artifact of the truncation error in the computed pixel position (Sigma-9). The same pathology occurs in the computation of low dispersion background fluxes, though in a round-about way: IUESIPS first computes the exact position of a background extraction slit. It locates the fractional positions of each pixel within this slit and proceeds to compute the flux by interpolating the fluxes bilinearly from four neighboring pixels. A typical ± 0.003 pixel discrepancy between the computers will translate into a different set of weights assigned to these four pixels by each computer, so that each machine

will report a different interpolated flux value. In our investigations of several low dispersion LWR images, we noticed that the pixel-to-pixel "granularity" of background pixels varied by nearly a factor of three across the spectral field. This granularity is the origin of the background flux discrepancy pattern.

"Pings" --

During readout of the LWR camera, an exponentially damped, sinusoidal noise pattern may be added to several lines of the raw image. This unwanted pattern arises from microphonics interference and has a periodicity of about 18 pixels. Its maximum amplitude is 20 DN in the raw image. During processing, the IUESIPS code flags the ping pattern and does not use the region affected in the background extraction. In a representative image with severe ping pattern, we found a rather slight enhancement (50%) of apparently random flux differences in the gross spectrum that propagate through to the net and absolute net spectra. This enhancement corresponds to the intersection of the ping lines with the spectrum in the original geometry, and slightly affects about 50A in the final spectra. As this enhancement is within the tolerance of ± 9 FN, it is of academic interest only.

The Wedge --

Early in the course of compatibility testing we discovered two wedge-shaped regions of the ELBL images which show relatively large flux discrepancies. Both wedges occur just inside the photometrically-corrected swath but outside the "science area" normally used in the extraction of background fluxes. As Figure 13 shows, the two wedges are located at the extreme upper and lower left of the ELBL rectangle. For this reason, the wedge may be of academic interest only to most I.U.E. investigators. The size of flux differences in the wedge areas is comparable to the pixel-to-pixel background differences, typically ± 300 FN. The "wedge" occurs because of the confluence of two unrelated idiosyncrasies, one of the Sigma-9 computer and the other the LWR camera. The two peculiarities come together in an unfortunate way in the computation of the low dispersion background flux in two corners of the ELBL rectangle. To understand this, recall that the ELBL file is created by rotating a portion of the PI image and arranging new rows of rotated pixels parallel to the direction of dispersion. At each wavelength, the center of the spectrum is located in geometrically correct space. An offset is then applied to determine the geometrically correct coordinates for each of the 110 pseudo-orders in the new ELBL file. These coordinates are then transformed to raw image space for extraction. Because of memory constraints in the Sigma-9, only 200 pixels are read for each PI-line needed. The specific 200 pixels are determined by approximating the location of the center of the spectral order using the adjusted dispersion constants and the raw image line. Usually, this segment of pixels is long

enough to include all pixels for which flux computations are made, but not always. When the segment is not long enough, the Sigma-9 incorrectly uses a flux value of a pixel from an earlier read cycle. Since the VAX does not read incomplete data segments, the flux difference between the two machines will be large. The wedge anomaly occurs only for the two corners of the ELBL image and only for the LWR camera. The reason for this lies in yet another peculiarity, this time of the reseau displacements, which are needed to map raw space coordinates to correct rectilinear coordinates. The equation referred to above to locate the spectrum-center along a PI line includes a mixture of dispersion constants (appropriate for geometrically-correct space), and the PI line number (appropriate to raw space). The use of mixed-geometrical parameters in an algebraic statement is tolerable when geometric distortions in the image are small. However, the geometric distortions in the line direction are abnormally large both in the upper and lower short-wavelength corners of the LWR camera image. Here the mixing of parameters from both geometries causes a poor estimate of the distance to the spectrum center. We find that in these two sections of the camera only (and not at all in the LWP and SWP cameras), the line segment fails to include the pixel of interest by 3-4 pixels. Consequently, the wrong flux is used in the computation of the ELBL flux at the particular coordinate. It should be emphasized that this problem never affects the science image. Additionally, it does not occur at all with the VAX-based IUESIPS.

SUMMARY

The discrepancies between Sigma-9 and VAX processing fall within the tolerances of real-number computational errors: the VAX rounds and the Sigma-9 truncates. Larger differences than expected occur in two small wedge-shaped areas outside the "science area" in low-dispersion, ELBL images. As a result of this analysis, the scientific staff of the IUE Observatory at Goddard has concluded that VAX vs. Sigma-9 processing differences have no substantial scientific impact. Accordingly, the reprocessing of LWR images will proceed per demand. Please note that the reprocessing of LWR images at VILSPA will continue with the Sigma-9 version of IUESIPS.

REFERENCES

Nichols-Bohlin, J. 1987, IUE Three-Agency Coordination Meeting, Madrid.

_____, 1988, NASA IUE Newsletter, 35, 29.

Treinish, L. 1980, NASA Tech Mem. 81995.

FIGURE CAPTIONS

Figure 1: Flux difference plot and histogram of order 92 for the gross high dispersion spectrum LWR 6257 between data processed by the Sigma-9 and by the VAX computers, respectively. In the top plot the y-axis is in flux units "FN"; the x axis is in Angstroms. The bottom plot is the frequency of occurrence (number of pixels) versus FN difference (only non-zero flux differences are represented). A discrepancy of 196 FN occurs at 2507A because the two computers assign this wavelength to neighboring pixels (2514A feature: same explanation). Although this discrepancy seems large, it is still small compared to the flux in the spectra themselves (25000 FN).

Figure 2: Flux difference plot and histogram of order 92 for the background high dispersion spectrum LWR 6257 between data processed by the Sigma-9 and by the VAX computers. A discrepancy of 2362 FN occurs at 2491A because the two computers assign this wavelength to neighboring pixels; 2000 FN is pixel-to-pixel noise variation. In the lower histogram non-zero differences only are plotted.

Figure 3: Flux difference plot and histogram of order 92 for the net high dispersion spectrum LWR 6257 between data processed by the Sigma-9 and by the VAX computers. Since the net spectrum is the difference of the gross and the smoothed background spectra, the "spikes" at 2507A and 2514A in Fig. 1 carry over into the top figure here. (Note that the 2491A spike in the background difference spectrum does not propagate here because of smoothing.) The slight negative slope in the differences reflects an accumulation of truncation errors in the Sigma-9 (see text).

Figure 4: Flux difference plot and histogram of order 92 for the ripple-corrected, "absolute net" flux for the high dispersion spectrum LWR 6257 between data processed by the Sigma-9 and by the VAX computers. Top plot: the "spikes" at 2507A and 2514A from Fig. 1 are propagated here. The tapering at the long-wavelength end of the difference plot is an artifact of the ripple correction imposed upon the continuum. The negative-FN "tail" of the histogram (lower plot) is a reflection of this tapering.

Figure 5: Flux difference plot for the gross low dispersion spectrum LWR 18150 between data processed by the Sigma-9 and by the VAX computers. As before, the y-axis represents flux in units of "FN"; the x-axis is in Angstroms. The off-scale "spike" at 2190A represents the amplification by a bright spot of small differences in pixel positions (typically ± 0.003 pixel) determined by the two computers; a steep flux gradient across adjacent pixels exaggerates the computational differences in pixel location.

Figure 6: Histogram for Fig. 5, of the flux differences for the gross low dispersion spectrum LWR 18150 between data processed by the Sigma-9 and by the VAX computers (only non-zero differences are represented).

Figure 7: Flux difference plot with wavelength for the background low dispersion spectrum LWR 18150 between data processed by the Sigma-9 and VAX computers. Note the strong dependence of the difference along the order. This change in amplitude is a reflection of the change in pixel-to-pixel "granularity" in the LWR camera (cf. Fig. 3 of Nichols-Bohlin, 1988).

Figure 8: Histogram for Fig. 6, of the flux differences for the background low dispersion spectrum LWR 18150 between data processed by the Sigma-9 and by the VAX computers.

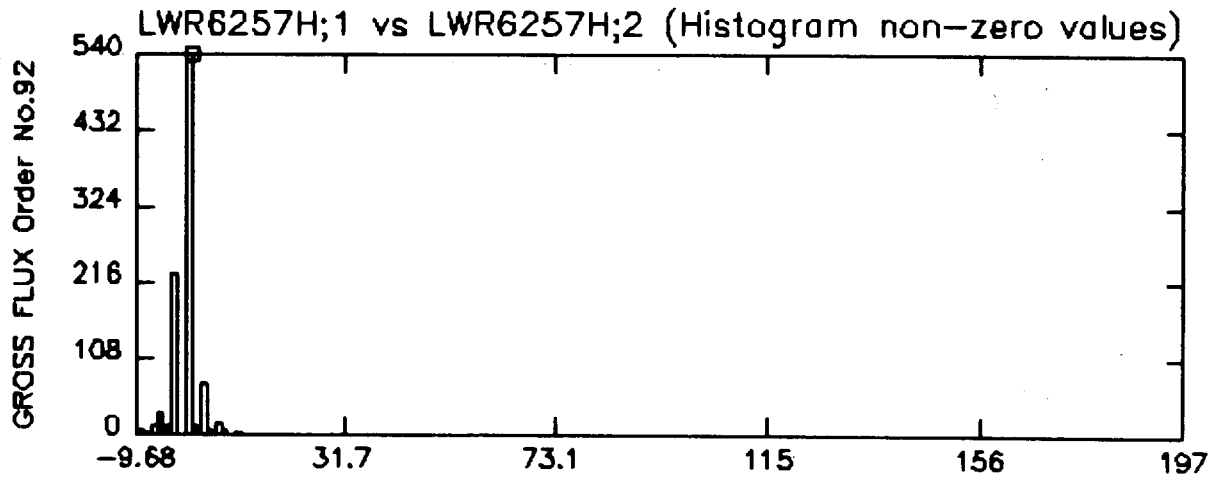
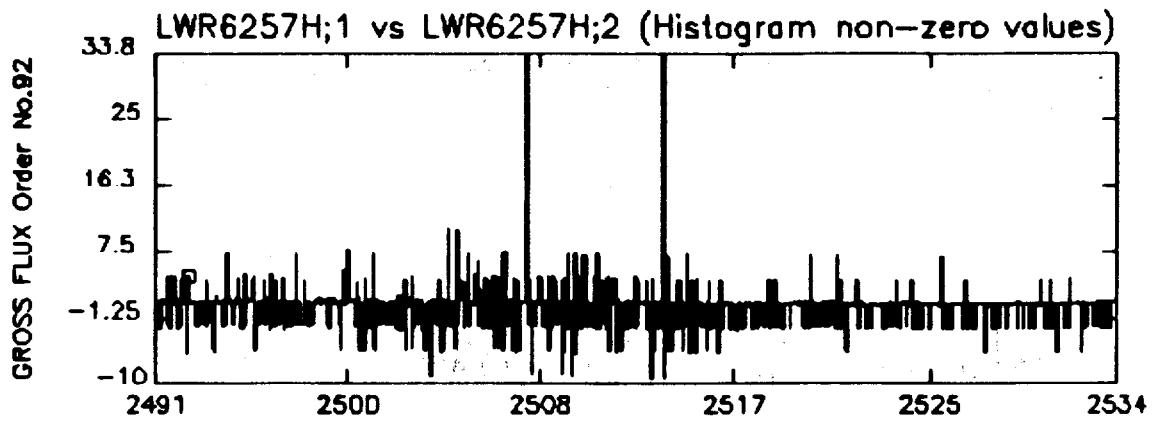
Figure 9: Flux difference plot with wavelength for the net low dispersion spectrum LWR 18150 between data processed by the Sigma-9 and VAX computers. The 2190A "spike" and change in fluctuation level are propagations from Figs. 5 and 7.

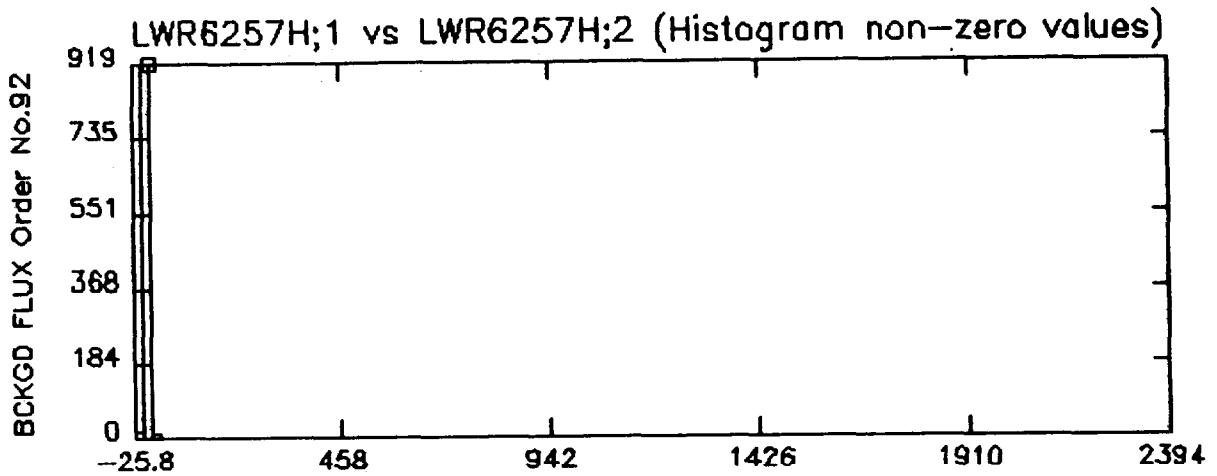
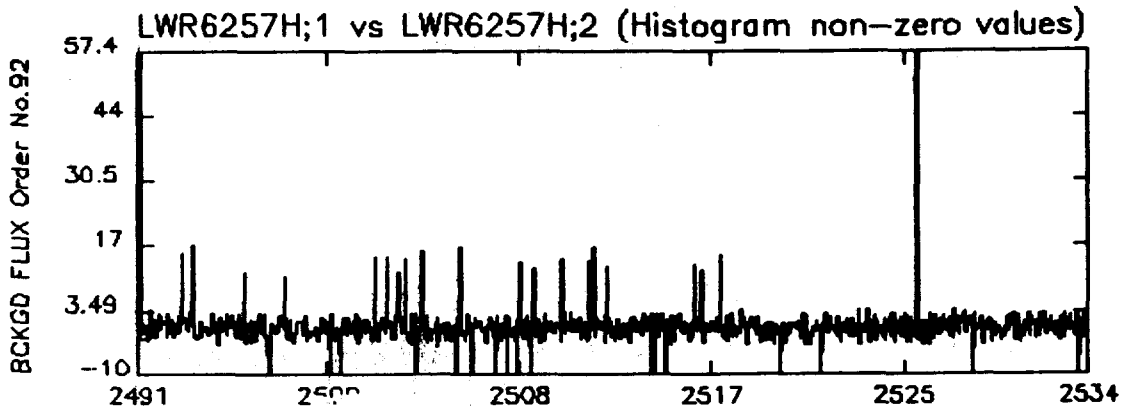
Figure 10: Histogram for Fig. 9, of the flux differences for the net low dispersion spectrum LWR 18150 between data processed by the Sigma-9 and by the VAX computers.

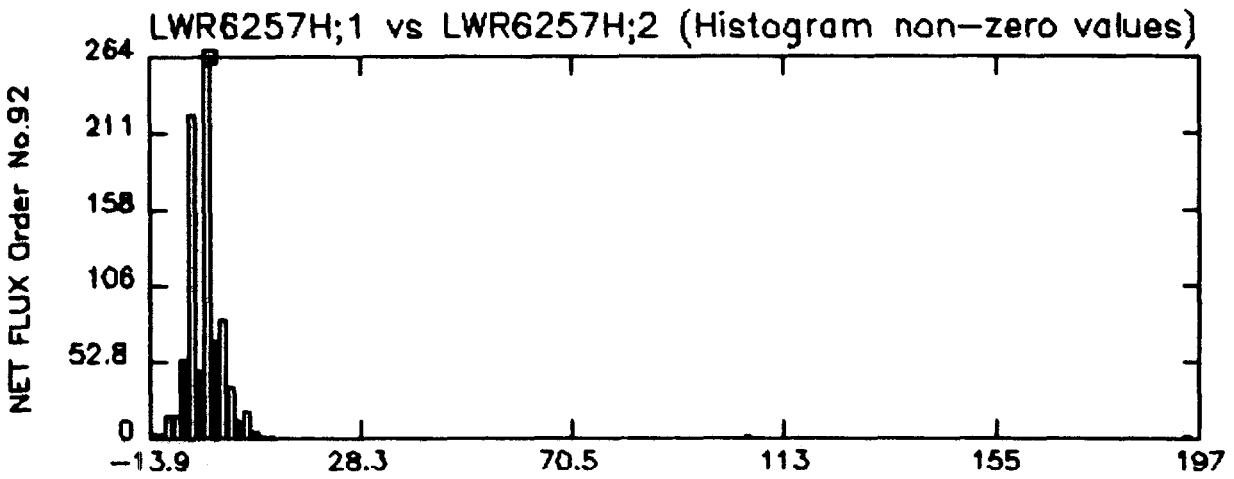
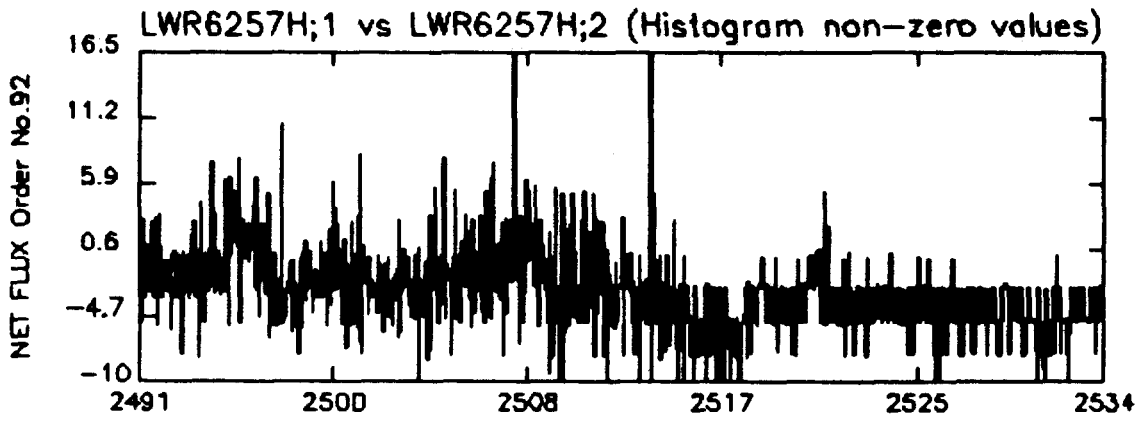
Figure 11: Flux difference plot with wavelength for the absolutely calibrated net low dispersion spectrum LWR 18150 between data processed by the Sigma-9 and VAX computers. The 2190A "spike" propagates from Fig. 5.

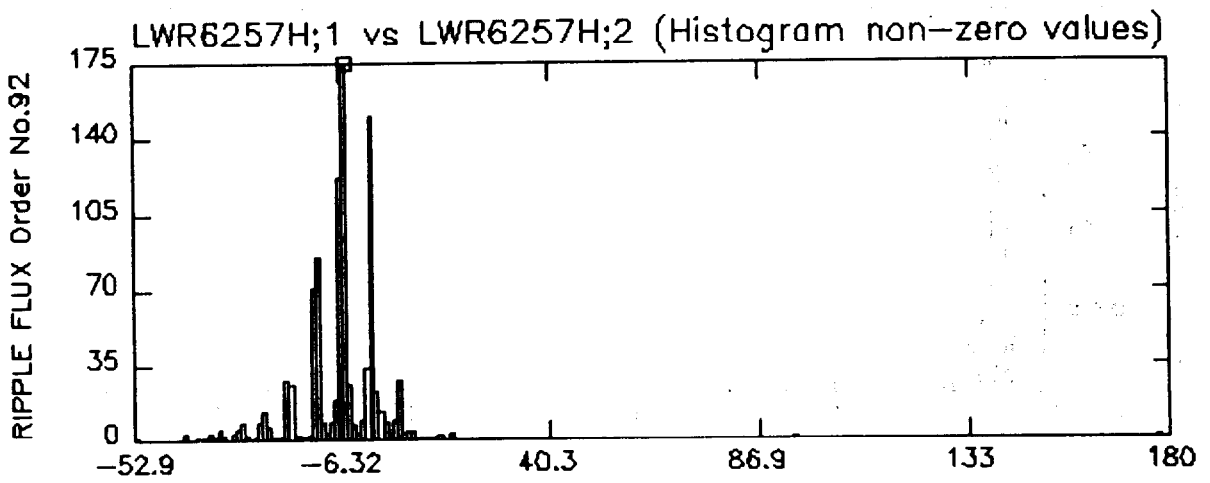
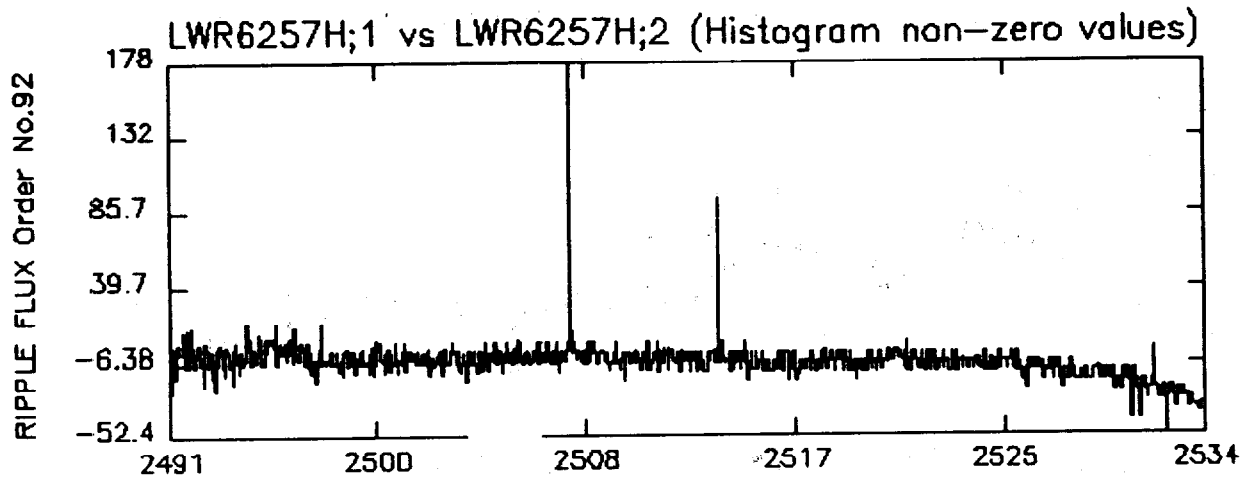
Figure 12: Histogram for Fig. 11, of the flux differences for the absolutely calibrated net low dispersion spectrum LWR 18150 between the Sigma-9 and VAX computers.

Figure 13: Picture of the flux differences of the ELBL, photometrically-corrected science-image for the low dispersion spectrum LWR 9981 between data processed by the Sigma-9 and VAX computers. Note the "wedge" shaped regions in the upper and lower left corners of the image where the flux differences are relatively large. (These wedges are outside the "science image" used by IUESIPS to extract the final MELO spectra.

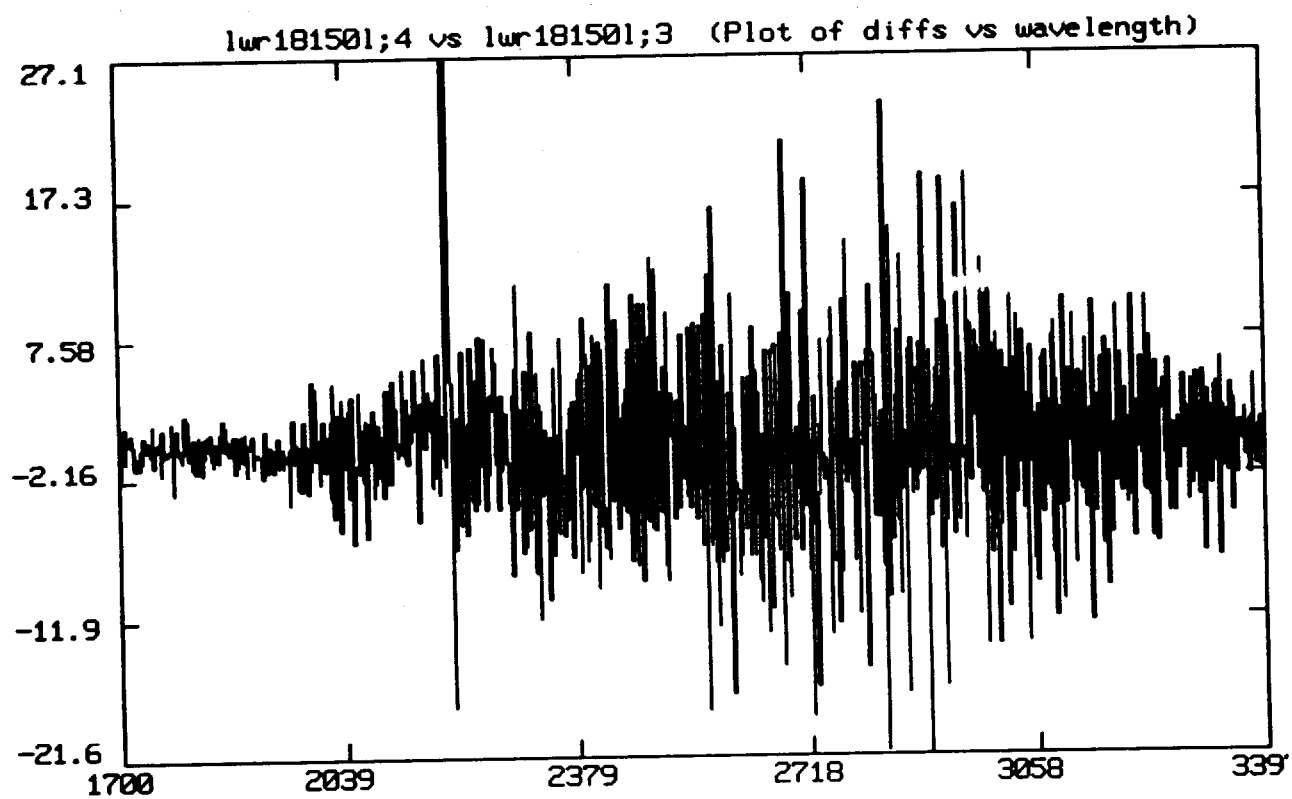




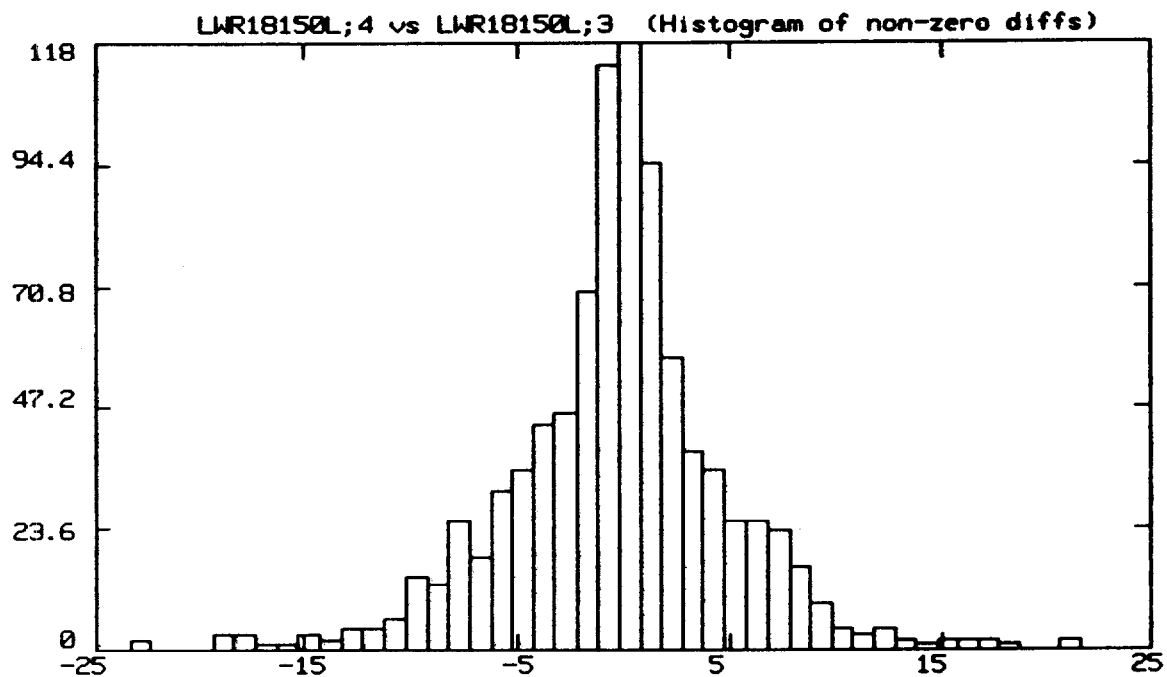




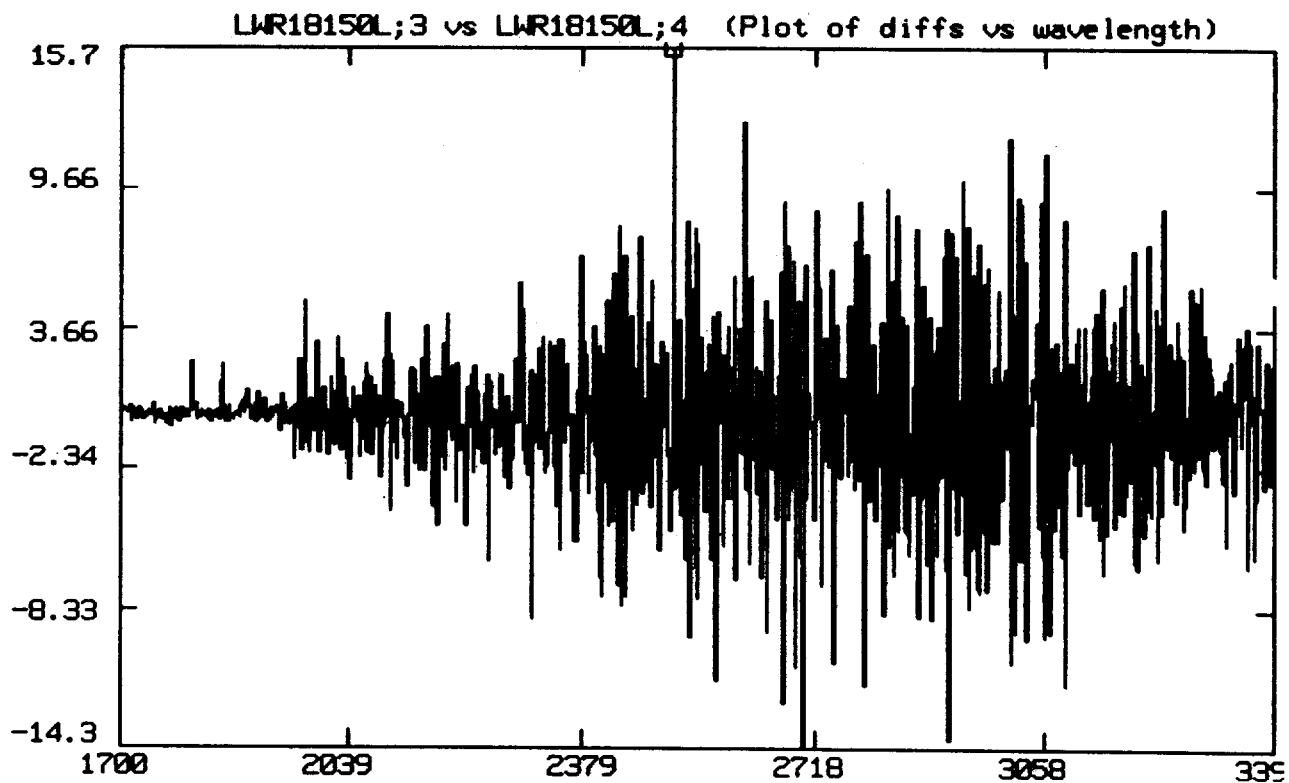
g,b,n or a flux difference vs. wavelength



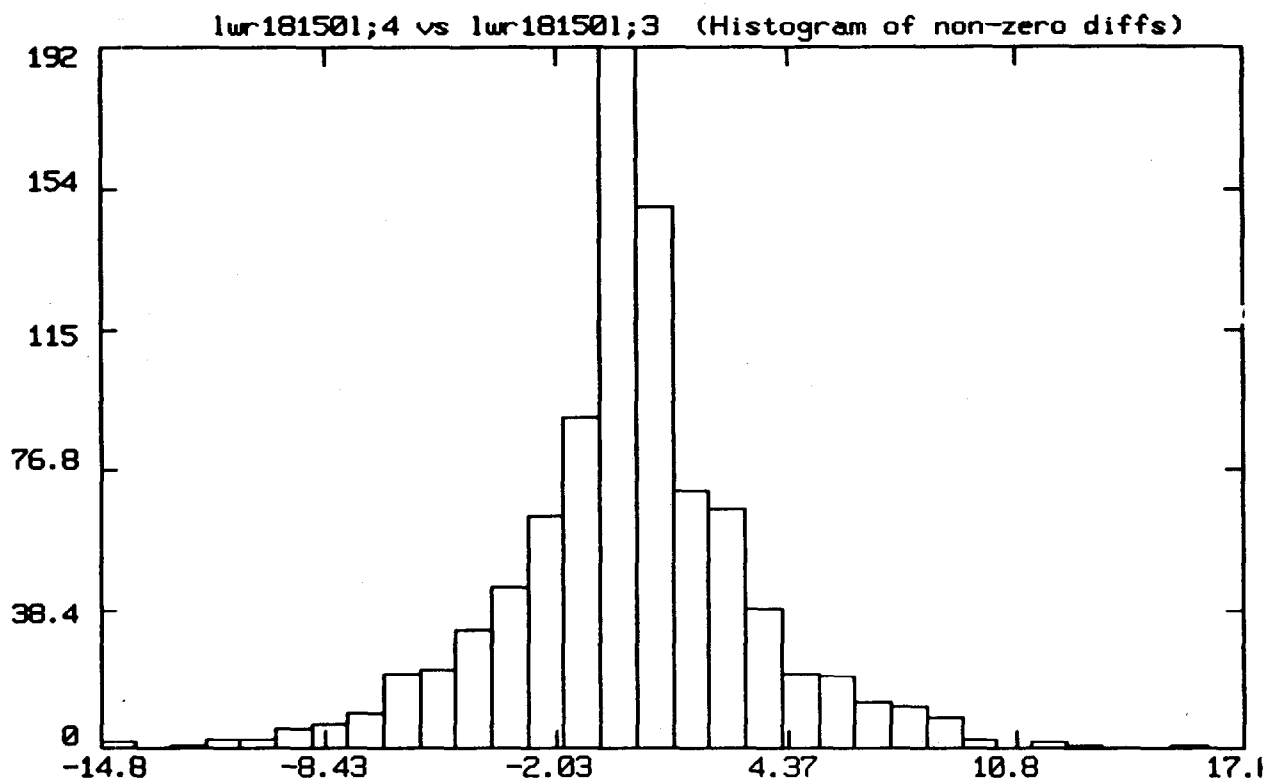
GROSS FLUX ORDER NO. 1 BIN WIDTH 1.0
Minimum Difference = -22.773
Maximum Difference = 432.48
1 out of 907 values were identical



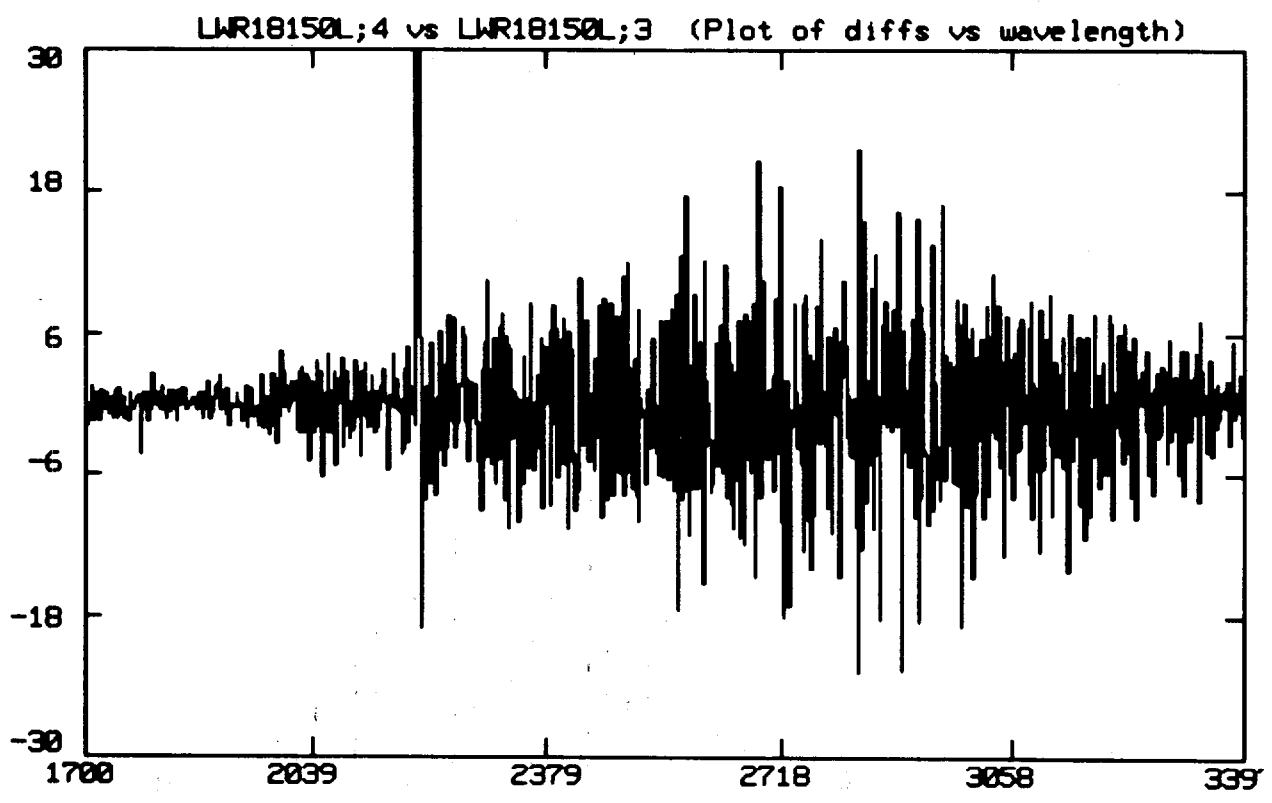
g,b,n or a flux difference vs. wavelength



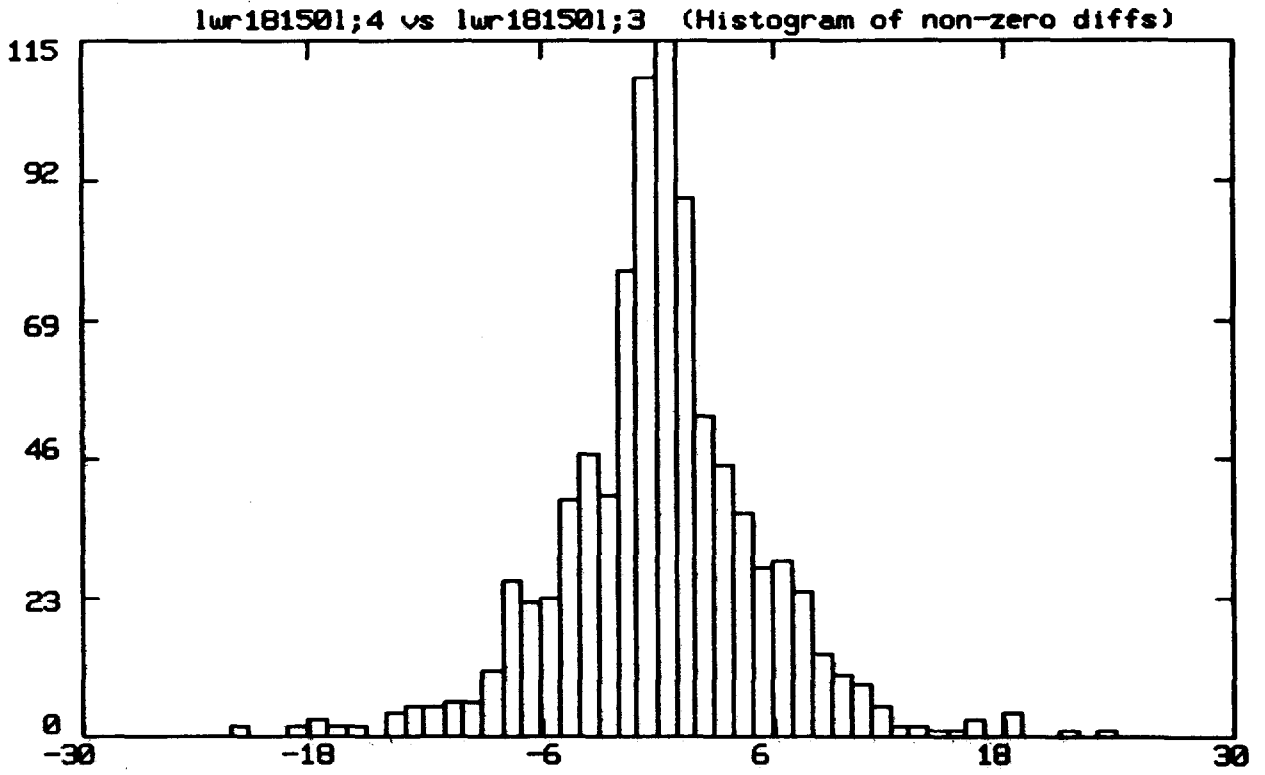
BACKGROUND FLUX ORDER NO. 1 BIN WIDTH 1.0
Minimum Difference = -14.333
Maximum Difference = 15.659
1 out of 907 values were identical



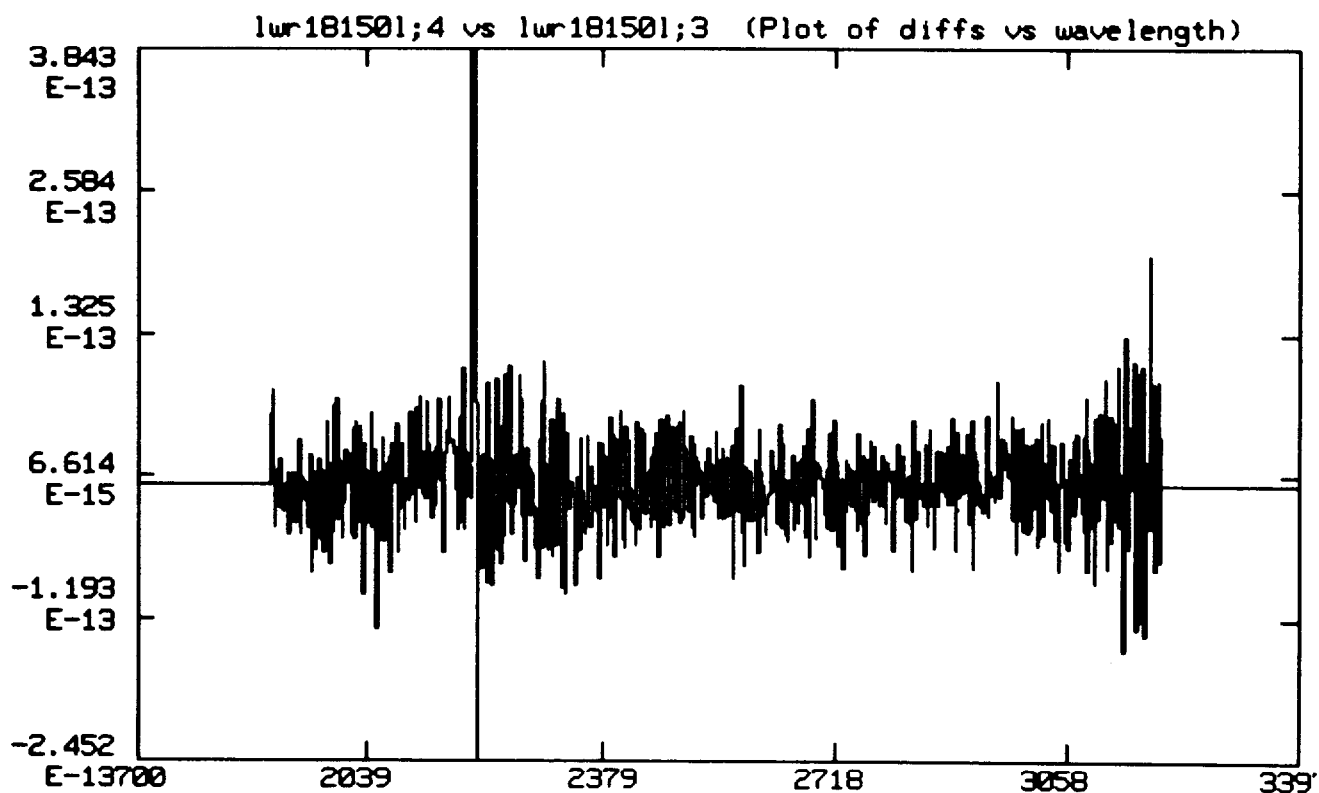
g,b,n or a flux difference vs. wavelength



NET FLUX ORDER NO. 1 BIN WIDTH 1.0
Minimum Difference = -21.629
Maximum Difference = 432.83
1 out of 907 values were identical



g,b,n or a flux difference vs. wavelength



ABS CALIB FLUX ORDER NO. 1 BIN WIDTH 0.0
Minimum Difference = $-2.45193\text{E-}13$
Maximum Difference = $6.14919\text{E-}12$
214 out of 907 values were identical

